

HORIZONTAL AND VERTICAL CO₂ ADVECTION IN A SLOPING FOREST

MARC AUBINET*, BERNARD HEINESCH and MICHEL YERNAUX
Unité de Physique des Biosystèmes, 8 avenue de la Faculté, B-5030 Gembloux, Belgium

(Received in final form 4 November 2002)

Abstract. A system measuring the horizontal and vertical advection was devised and installed in a sloping forest at the Vielsalm site, Belgium. The measurements showed that under stable conditions a flow regime established below the canopy: air flowed horizontally along the slope and entrained the air above the canopy vertically. This movement occurs during stable nights characterised by strongly negative net radiation. It creates negative air concentration gradients in both the vertical and horizontal directions. The advection fluxes associated with these movements are opposite and of a similar order of magnitude. This implies that the horizontal advection cannot be ignored in the carbon budget equation at night. Unfortunately, the large variability of, and considerable uncertainty about, advection fluxes does not enable one to produce estimates of the source term from these equations. Advection measurement systems should be improved in order to enable such estimates to be made. Particular attention should be paid to the estimation of the vertical velocity above the canopy and to the vertical profiles of the horizontal velocity and horizontal CO₂ gradient below the canopy.

Keywords: Advection, CO₂, Forest, Night flux.

1. Introduction

Since the development of regional and global networks (CARBO-EUROFLUX, AMERIFLUX, LBA, ASIAFLUX, FLUXNET), many long-term measurements of the CO₂ net exchange between forests and atmosphere (Net Ecosystem Exchange, NEE) have been performed (Wofsy et al., 1993; Goulden et al., 1996; Greco and Baldocchi, 1996; Black et al., 1996; Valentini et al., 2000). They have been carried out by measuring the turbulent eddy flux above the forest canopy using an eddy covariance system (Moncrieff et al., 1997; Aubinet et al., 2000), and the CO₂ storage below the measurement point using infrared gas analysers. This 'eddy covariance' method is based on the assumption that the NEE is equal to the sum of these two fluxes. It ignores the other terms of the mass conservation equation and, in particular, the advection terms. This approximation is formally correct if the flow and the scalar fields are horizontally homogeneous. These conditions are not encountered in most of the forested sites, however, because of non-flat terrain, heterogeneity of land-surface cover or mesoscale circulations. The problem is particularly critical during stable nights when most of the assumptions supporting the eddy covariance

* E-mail: aubinet.m@fsagx.ac.be



methodology are not satisfied. In these conditions, under-evaluation of the CO₂ fluxes using the eddy covariance method frequently occurs (Goulden et al., 1996; Black et al., 1996; Lee et al., 1997; Baldocchi et al., 1997; Lindroth et al., 1998; Aubinet et al., 2000). Several reasons may explain this underestimation – the loss of high frequency fluxes by the eddy-covariance instrumentation, loss of low frequency fluxes caused by using low pass data filters that are too short, and incorrect measurement of CO₂ storage in the air and the soil (Mahrt, 1998; Aubinet et al., 2000; Massman and Lee, 2001; Turnipseed et al., 2002). There is more and more evidence, however, indicating that the night flux underestimation is due mainly to the neglect of advection processes rather than to measurement errors.

As the night flux error acts as a selective systematic error (Moncrieff et al., 1996), its impact on the net CO₂ exchange and on the estimation of the carbon sequestration by the forest is quantitatively important. Based on the most commonly used turbulence correction for night fluxes (Goulden et al., 1996), the relative impact on the annual carbon sequestration of the nighttime error varies from a few percent (Pilegaard et al., 2001) to 50% (Schmid et al., 2001), depending on the site. The part of the error that can be explained by the storage varies from 5 to 35%, depending on the site (Aubinet et al., 2000). At the Vielsalm site, where the current experiment was carried out, the impact of the nighttime error varied from 10 to 20%, depending on the year (Aubinet et al., 2002).

The objective of this study is to understand the mechanisms that control the air flows at the Vielsalm site under stable conditions. This analysis is simplified by the particular topography of the site: The uniform and gentle slope at the site favours the development of gravity flows in the slope direction. Consequently, it is reasonable to assume that the air flow pattern is mainly two dimensional (2D) during these periods, and thus a system collecting air velocity and CO₂ concentration in a two-dimensional form was installed at the site over a 3-month period. These measurements were analysed in order to understand the air flow pattern that develops at the site under stable conditions and to estimate the order of magnitude of the advection flux. The uncertainties on advection flux measurements were also discussed and recommendations for further research were given.

2. Theory

The conservation equation of a scalar in a control volume may be written (Finnigan, 1999):

$$\begin{aligned} & \frac{1}{2L} \int_0^h \int_{-D}^D S(t, x, z) dx dz \\ &= \frac{1}{2L} \int_0^h \int_{-D}^D \frac{1}{V_m} \left(\frac{\partial \bar{c}}{\partial t} + \frac{\partial \bar{u}\bar{c}}{\partial x} + \frac{\partial \bar{u}'c'}{\partial x} + \frac{\partial \bar{w}\bar{c}}{\partial z} + \frac{\partial \bar{w}'c'}{\partial z} \right) dx dz, \end{aligned} \quad (1)$$

where $x_i \equiv x, y, z$ is a right-handed coordinate system with x in the mean stream-wise direction, y in the cross-stream lateral direction, and z in the surface normal direction, $u_i \equiv u, v, w$ are the wind velocity components in this coordinate system, overbars are time averages, primes are fluctuations around the average, V_m is the molar volume of dry air, c is the mixing ratio with respect of dry air of the scalar and S is the source term. For simplicity, lateral homogeneity is assumed so that the volume may be restricted to a two-dimensional box along the x and z axes. The upper boundary of the box is in the air at the height of the eddy covariance measurement system (h), lateral boundaries are in the air at horizontal distances D upstream and downstream to the measurement tower, and the lower boundary is at soil level. If, in addition, the vertical integral of $\partial \bar{c} / \partial t$ on the tower is considered to be representative of the control volume and the sonic is supposed to be placed at a height h higher than a blending height h_b above which the horizontal variation in vertical fluxes can be neglected, Equation (1) can be written:

$$\begin{aligned}
 & \frac{1}{2L} \int_0^h \int_{-D}^D S(t, x, z) dx dz + \frac{1}{V_m} (\overline{w'c'})_0 \\
 &= \int_0^h \frac{1}{V_m} \left(\frac{\partial \bar{c}}{\partial t} \right) dz + \frac{1}{V_m} (\overline{w'c'})_h \\
 &+ \frac{1}{2L} \int_0^h \int_{-D}^D \frac{1}{V_m} \left(\frac{\partial \bar{u}\bar{c}}{\partial x} + \frac{\partial \bar{w}\bar{c}}{\partial z} \right) dx dz \\
 &+ \frac{1}{2L} \int_0^h \int_{-D}^D \frac{1}{V_m} \left(\frac{\partial \overline{u'c'}}{\partial x} \right) dx dz. \tag{2}
 \end{aligned}$$

The two terms on the LHS of Equation (2) represent the source or the sink of CO₂ due to the assimilation or the respiration of the soil and the canopy elements in the control volume. The first term on the RHS represents the storage term below the measurement point, the second term is the vertical eddy flux at the measurement point, the third term represents the advection and the fourth term, the horizontal divergence of the turbulent flux. In current practice, the sites are considered to be sufficiently homogeneous to allow one to neglect the two last terms. This is, however, not proven as these terms are difficult to estimate accurately because of the difficulty of measuring vertical velocity \bar{w} , horizontal CO₂ gradient $\partial \bar{c} / \partial x$ and horizontal $\overline{u'c'}$ divergence. Recently, Lee (1998) proposed a method to estimate the vertical advection term from single tower measurements. Postulating horizontal homogeneity, i.e., $\bar{c}(x, z)$, he proposed writing the third term of RHS of Equation (2) as:

$$\frac{1}{2L} \int_0^h \int_{-D}^D \frac{1}{V_m} \left[\frac{\partial \bar{u}\bar{c}}{\partial x} + \frac{\partial \bar{w}\bar{c}}{\partial z} \right] dx dz = \frac{1}{2L} \int_0^h \int_{-D}^D \frac{1}{V_m} \left[\bar{c} \frac{\partial \bar{u}}{\partial x} + \frac{\partial \bar{w}\bar{c}}{\partial z} \right] dx dz. \tag{3}$$

By combining (3) with the continuity equation

$$\frac{\partial \bar{u}}{\partial x} = -\frac{\partial \bar{w}}{\partial z}$$

and integrating it, this becomes:

$$\frac{1}{2L} \int_0^h \int_{-D}^D \frac{1}{V_m} \left[\frac{\partial \bar{u} \bar{c}}{\partial x} + \frac{\partial \bar{w} \bar{c}}{\partial z} \right] dx dz = \int_0^h \frac{1}{V_m} \left[-\bar{c} \frac{\partial \bar{w}}{\partial z} + \frac{\partial \bar{w} \bar{c}}{\partial z} \right] dz, \quad (4)$$

and, after introducing the hypothesis

$$\frac{\partial \bar{w}}{\partial z} = \frac{\bar{w}_h}{h},$$

$$\frac{1}{2L} \int_0^h \int_{-D}^D \frac{1}{V_m} \left[\frac{\partial \bar{u} \bar{c}}{\partial x} + \frac{\partial \bar{w} \bar{c}}{\partial z} \right] dx dz = \frac{1}{V_m} \bar{w}_h (\bar{c}_h - \langle c \rangle), \quad (5)$$

where

$$\langle c \rangle = \frac{1}{h} \int_0^h \bar{c}(z) dz.$$

With these hypotheses, in addition to the neglect of the horizontal divergence of the turbulent flux, Equation (2) finally becomes:

$$NEE = \int_0^h \frac{1}{V_m} \left(\frac{\partial \bar{c}}{\partial t} \right) dz + \frac{1}{V_m} (\overline{w'c'})_h + \frac{1}{V_m} \bar{w}_h (\bar{c}_h - \langle c \rangle). \quad (6)$$

The expression (6) has been used in several studies (Lee, 1998; Baldocchi et al., 2000; Paw U et al., 2000) to derive estimations of NEE that take account of the vertical advection. Its advantage is that the advection estimation is based on only one point of measurement. It supposes however that the horizontal advection and the horizontal divergence of the turbulent flux are negligible, which is not justified theoretically (Finnigan, 1999; Finnigan et al., 2003). In particular Finnigan (1999) suggested the horizontal advection to be of the same order of magnitude as the vertical advection. In this paper, we will concentrate on the advection terms. Our analysis will be based on an alternative budget equation that is based on (2), uses the Lee approach for the vertical advection but takes into account the horizontal advection term. It writes:

$$\begin{aligned} NEE = & \int_0^h \frac{1}{V_m} \left[\frac{\partial \bar{c}}{\partial t} \right] dz + \frac{1}{V_m} (\overline{w'c'})_h \\ & + \frac{1}{V_m} \bar{w}_h (\bar{c}_h - \langle c \rangle) + \int_0^h \frac{1}{V_m} u(z) \frac{d\bar{c}}{dx} dz. \end{aligned} \quad (7)$$

The horizontal advection term depends on the horizontal CO₂ concentration gradient whose estimation requires at least two points of measurement. The analysis that follows is based on the latter equation. In this paper, we will use the sign convention, currently used in the eddy flux community, that the positive vertical direction is upward and the positive horizontal direction is in the mean flow direction. Consequently, a positive advection flux will be associated with an emission of CO₂ from the control volume and a negative advection with an accumulation of CO₂ in the control volume.

3. Material and Methods

3.1. SITE

The study site is in Vielsalm in the Belgian Ardennes (50° 18' N , 6° 00' E, altitude 480 m ASL) on the side of an open valley (440 to 560 m). The slope is uniform, in a north-westerly direction, and of the order of 3% (Figure 1a). The site provides a fetch of 1500 m in a south-westerly direction and 500 m in a north-easterly direction; these are the most frequently observed wind directions in daytime conditions. A clearcut (a tree nursery of about 5 ha) limits the fetch in the upslope direction to 250 m. Beyond the clearcut, the forests extents on more than 3 km. The stand is of mixed composition, comprising Douglas fir (*Pseudotsuga menziesii* (Mirb.) Franco), beeches (*Fagus sylvatica* L.), silver fir (*Abies alba* Miller), Norway spruce (*Picea abies* (L.) Karst.), Scots pine (*Pinus sylvestris* L.) and pedunculate oak (*Quercus robur* L.). The leaf area index of the canopy is 5.0. The undercover is very sparse in the conifer sub-plot and non-existent in the beech sub-plot. A more complete description of the site is given by Laitat et al. (2000).

3.2. MEASUREMENTS

A measurement system was installed at the site to provide half-hourly averages of fluxes as well as standard meteorological data. It consisted of an eddy covariance system and an automated meteorological station. The eddy covariance system was the standard system used in the EUROFLUX network, and consisted of a fast response infrared gas analyser (IRGA) (model LI-6262, LI-COR Inc., Lincoln, NE, USA) and a three-dimensional sonic anemometer (model SOLENT 1012R2, Gill Instruments, Lymington, U.K.). It was placed on a 40-m-high tower. The system and measurement procedure was described in detail by Aubinet et al. (2000, 2001). The micrometeorological and flux measurements were also described by Aubinet et al. (2001, 2002). In addition to the fluxes, the eddy covariance measurements at 40 m were used in order to give an estimate of the boundary-layer thermal stability. The sonic anemometer of the eddy covariance system was also used to estimate the vertical component of the velocity at the top of the tower.

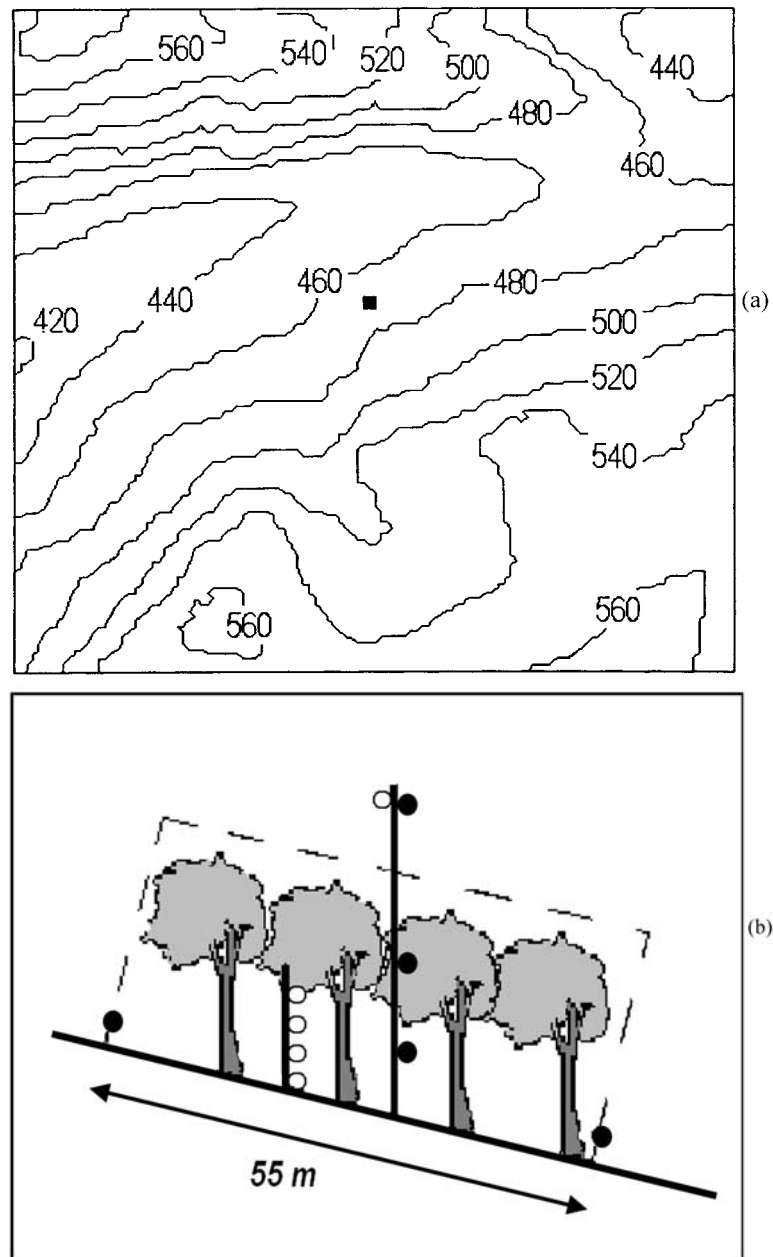


Figure 1. Site description. (a) Topographical map of the site (3 km \times 3 km). The tower is represented by a black square. Contour labels are in metres and each contour represents 20 m. (b) Representation of the experimental set-up. Location of the sonic anemometers are represented by the open points. CO₂ sampling points are represented by the black points.

In addition to this set-up, a system devised to estimate the advection fluxes was installed for 3 months during summer 1999. It measured the CO₂ concentration of the air and the horizontal velocity at several points below the eddy covariance sensor (Figure 1b). Estimates of the air CO₂ concentrations were produced half hourly at 8, 22 and 36 m on the tower and at a height of 1 m at two locations 55 m apart in the slope direction. Each estimation was made by averaging 11 successive measurements taken every 2 min for the horizontal profile or deduced directly from one measurement for the vertical profile. The tubes were copper (vertical profile) and nylon (horizontal profile). All concentrations were measured using the same infrared gas analyser (WMA-2, PP systems), and this was automatically calibrated every 24 hrs. As the IRGA was not equipped with a pressure transducer, the tubing system was devised so as to avoid any systematic errors arising from pressure drops in the IRGA chamber. It used two pumps, one (KNF N86KN18, Village Neuf, France) to transport the air at a high flow rate from the sampling point to a reservoir maintained at the atmospheric pressure, and the other to sub-sample the air at a lower rate from the reservoir to the IRGA.

Horizontal velocity was measured at four heights (1, 2, 3 and 4 m) with home-made sonic anemometers. These 2D anemometers provided a path length of 0.60 m, a working frequency of 3 Hz and a proper dimension to avoid significant distortion of the flow field. They were calibrated through comparison with the SOLENT R2 anemometer and performed well for mean wind velocities (down to less than 0.05 m s⁻¹). More details on the system were given by Wang et al. (1999).

3.3. METHODS: ESTIMATE OF THE ADVECTION

3.3.1. *Vertical Advection*

The vertical advection term (third term of RHS in Equation (7)) was deduced from the vertical CO₂ profile and the vertical air speed at the tower top. Corrections for the sensor tilt were applied to the raw velocity using the procedure proposed by Lee (1998), Paw U et al. (2000) and Wilczak et al. (2000). This method consisted of applying a fixed angle rotation in the $u-w$ plane (β) that is based on the long-term estimation of the measurements. As this angle was supposed to depend mainly on the site topography and the instrument bias, it is assumed to be a function of the wind direction only (azimuthal angle α). It is therefore estimated by fitting a sinusoidal regression on the $\beta(\alpha)$ graph and making the hypothesis that β (and thus $\bar{\omega}$) was zero over a long period for all wind directions. In order to reduce the spread of β estimates, only periods of near-neutral stratification were selected (Finnigan, 1999).

3.3.2. *Estimate of the Horizontal Advection*

The estimate of the horizontal advection flux is based on the hypothesis that, during stable nights, the average of the horizontal velocities measured at 1, 2, 3 and 4 m, $\langle u \rangle$, and the horizontal CO₂ concentration gradient measured at 1 m, $\Delta \bar{c}_1 / \Delta x$, are

representative of the corresponding variables in the whole vertical profile. This assumption could be written:

$$\frac{\Delta c}{\Delta x} = \frac{\Delta \bar{c}_1}{\Delta x} f_c(z), \quad (8a)$$

$$u(z) = \langle u \rangle f_u(z), \quad (8b)$$

where the functions $f_c(z)$ and $f_u(z)$ characterise the shapes of the vertical profiles of the variables. These hypotheses are supported by the good repeatability of the observation during stable conditions. In addition, complementary observations made at different heights, during a further experiment in summer 2002, confirmed that this hypothesis holds in the trunk space. Consequently, the last term of RHS in Equation (7) may be written:

$$\int_0^h \frac{1}{V_m} u(z) \frac{d\bar{c}}{dz} dz = \frac{1}{V_m} \langle u \rangle \frac{\Delta \bar{c}_1}{\Delta x} \int_0^h f_u(z) f_c(z) dz = \frac{1}{V_m} \langle u \rangle \frac{\Delta \bar{c}_1}{\Delta x} h', \quad (9)$$

where h' is a scaling height, depending on the profile functions following:

$$h' = \int_0^h f_u(z) f_c(z) dz. \quad (10)$$

The experimental set-up used in this experiment is not sufficient to determine the exact value of the scaling height. However, the measurement campaign developed in summer 2002 investigated more completely the vertical profiles and suggested it to vary between 3 and 10 m.

4. Results

4.1. WIND VELOCITIES

The resultant horizontal wind vectors at 2 and 40 m were computed for three classes of stability and eight classes of the 40-m-height wind direction (Figure 2). The stability parameter is computed as z/L where L is the Obukhov length. It is clear that, under stable conditions, the wind regime below the canopy is decoupled from that above the canopy. Indeed (Figures 2e, f), the resultant wind vector at 2 m is oriented in the slope direction (south-east to north-west) regardless of the above-canopy wind direction. This suggests that under stable conditions the surface wind regime is dominated by downslope air movements that are independent of the above-canopy (ambient) wind speed. This is in contrast with unstable and near-neutral conditions where resultant wind vectors at 2 and 40 m correspond fairly closely, indicating a good coupling between the above- and below-canopy wind regimes (Figures 2a–d).

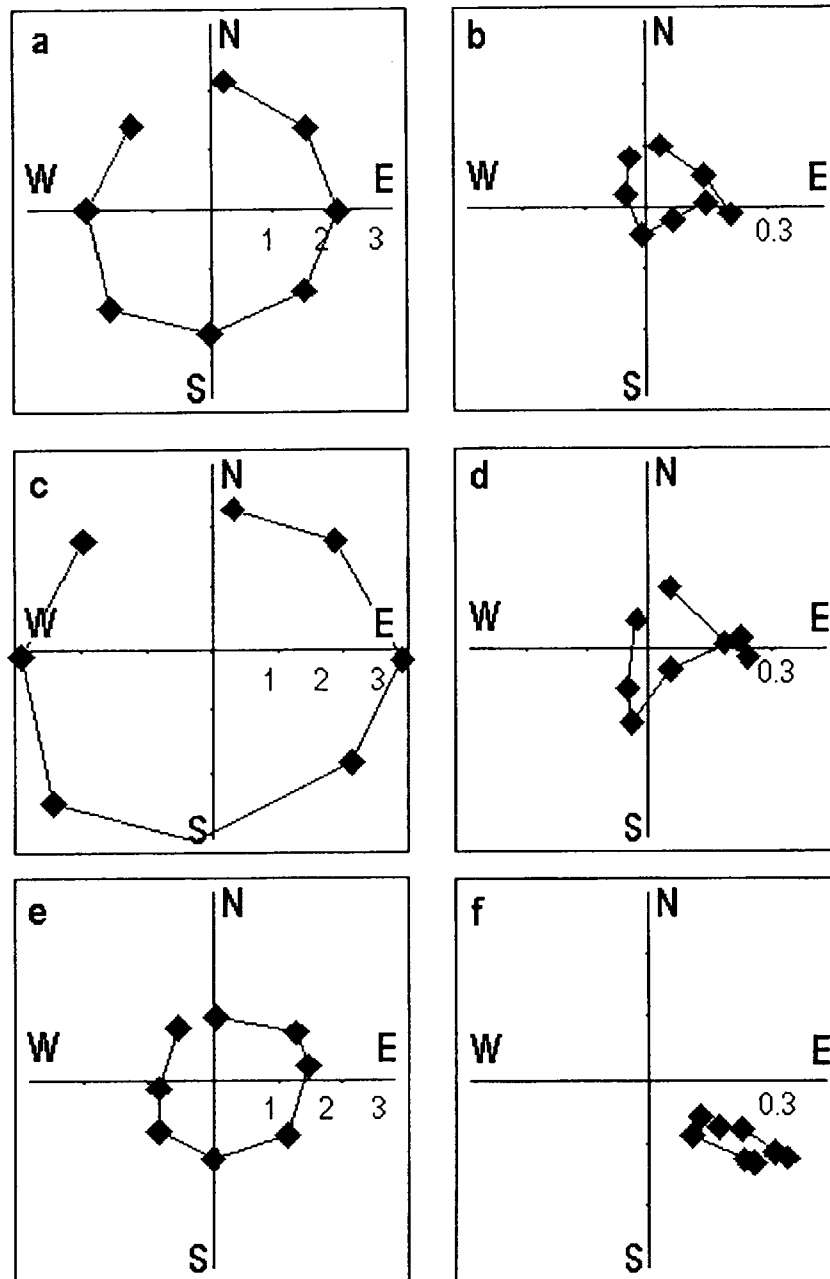


Figure 2. Resultant wind vectors (speed in m s^{-1}) computed for 8 direction classes of the 40-m-high wind direction ($337.5^\circ\text{--}022.5^\circ$, $22.5^\circ\text{--}067.5^\circ$, $067.5^\circ\text{--}112.5^\circ$, $112.5^\circ\text{--}157.5^\circ$, $157.5^\circ\text{--}202.5^\circ$, $202.5^\circ\text{--}247.5^\circ$, $247.5^\circ\text{--}292.5^\circ$, $292.5^\circ\text{--}337.5^\circ$) and for 3 classes of stability. 0° corresponds to North. The stability classes are: $z/L < -0.05$ (a, b), $-0.05 < z/L < 0.05$ (c, d), $z/L > 1$ (e, f). (a, c and e): Wind velocity above the canopy (40 m high). (b, d and f): Wind velocity below the canopy (average of four measurements taken at 2, 4, 6 and 8 m).

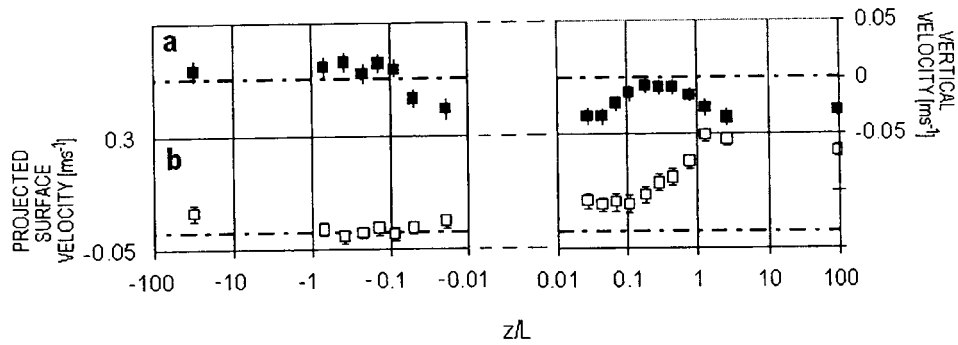


Figure 3. Evolution with stability of the vertical velocity above the canopy (a) and of the projected surface velocity (b). All the measurements are considered. Each point corresponds to an average of 200 measurements. The error bars represent the standard error of the mean.

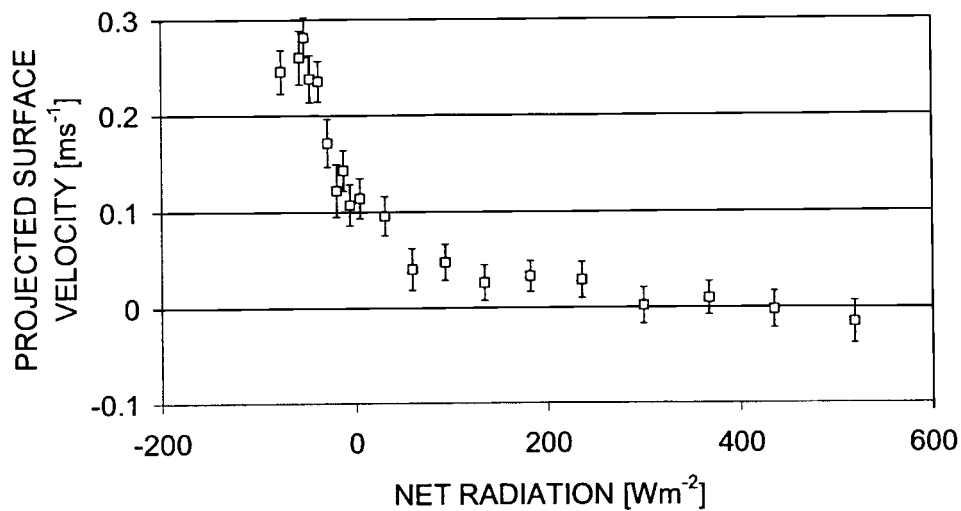


Figure 4. Evolution of the projected surface wind speed with net radiation. Each point corresponds to an average of 200 measurements. The error bars represent the standard error of the mean.

Another view of the surface velocity pattern under stable conditions is given in Figure 3 where the evolution of the slope projected horizontal velocity (u_{bproj}) with the stability is shown (open symbols). In the unstable range u_{bproj} is close to zero, confirming that the surface velocity has no privileged direction. In stable conditions it becomes increasingly positive, values up to 0.25 or 0.3 m s^{-1} being obtained for $z/L > 1$. The gravity flows are probably initiated by radiative cooling, which is confirmed by Figure 4, which shows a good correlation between u_{bproj} and net radiation under stable conditions. As the canopy is closed (LAI = 5), however, the radiative cooling that would be responsible for such flow cannot be exerted locally at the soil surface. It is more likely to take place in clearings situated upward of the site of measurement.

Gravity flows over slight slopes have not been frequently observed and described in the literature. Mahrt and Larsen (1990) studied the gravity flows on a sea shore and their results were similar to those of the current study. They also found that the surface and the ambient flow interact and, in particular, that upslope ambient winds could sometimes prevent the development of the gravity flow. Some interaction between the ambient and the surface flow also occurred in the current study, but to a smaller extent. Figure 2e shows that the surface wind speed depends on the ambient wind direction, lower values being observed when it is upslope (0.15 m s^{-1}) and higher values (0.4 m s^{-1}) when it is downslope. The lower interaction is probably because the presence of the canopy limits the interaction between the ambient and the surface flow.

The evolution with stability of the average vertical velocity above the canopy, w_h , is also shown in Figure 3 (closed symbols). It is characterised by two negative peaks, one in the near-neutral range, the other in the stable range; the origins of these two peaks are different. This appears clearly when looking at the evolution of w_h with the ambient velocity in each range (Figure 5); w_h increases with ambient velocity in the near-neutral range (Figure 5a) while it decreases with it in the stable range (Figure 5b). The increase of w_h with ambient velocity in the near-neutral range suggests that the near neutral peak probably results from an incomplete tilt correction, the sonic being not perfectly in alignment with the streamlines. This point will be detailed in the measurement error section and we will show in Annex A that the tilt error should indeed induce an error on w_h that increases with the ambient velocity. The peak at $z/L > 1$ has a different origin, and could be related to the gravity flow as suggested by the good correlation between the vertical velocity and the surface horizontal velocity (Figure 6). Our hypothesis is that the link between the two variables is explained by an entrainment mechanism: the air above the canopy is entrained by the gravity flow, which provokes a vertical downward movement. Entrainment processes have been observed in different flow patterns such as one- or two-dimensional jets and plumes (Lee and Emmons, 1961; Kotsovinos and List, 1977) or gravity flows (Manins and Sawford, 1979). These authors proposed a parameterisation of this process that assumed w_a was proportional to $u_{b\text{proj}}$, and the proportionality constant depended mainly on the Richardson number. They found the order of magnitude of this constant to be about 0.1 or less. The slope of the relationship between w_a and $u_{b\text{proj}}$ in Figure 6 is of the same order of magnitude, which supports this hypothesis. If real, the entrainment process should induce an increase in the horizontal flow with the distance along the slope and thus an increase in either the height of the layer concerned with the drainage flow or the average horizontal velocity. As our measurement system included only one vertical profile of horizontal velocity, we could not check this hypothesis.

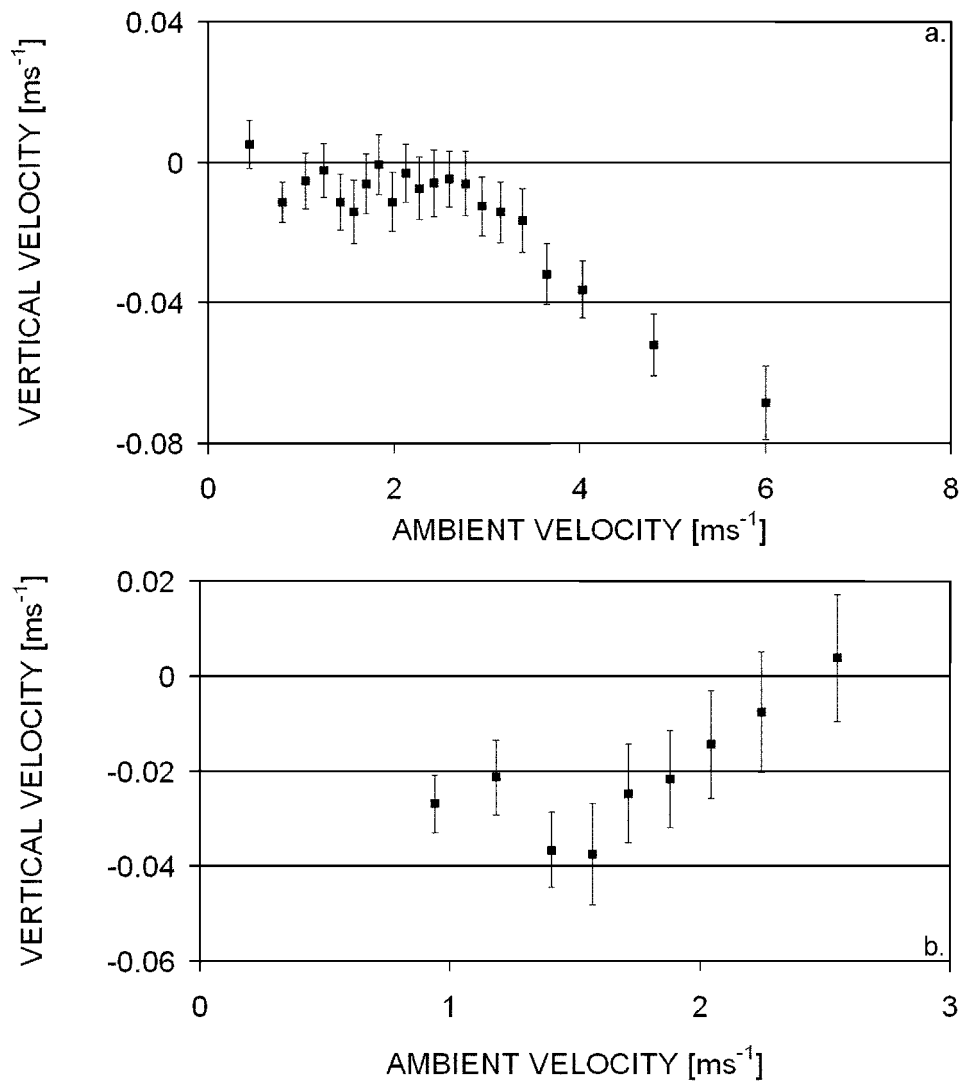


Figure 5. Evolution of the vertical velocity above the canopy with the ambient velocity. (a) In the near-neutral range ($-0.1 < z/L < 0.1$). Each point corresponds to an average of 100 measurements. (b) In the stable range ($z/L > 0.3$). All the measurements are considered. Each point corresponds to an average of 200 measurements. In both figures, the error bars represent the standard error of the mean.

4.2. CONCENTRATION GRADIENTS AND ADVECTION

The evolution with stability of the nighttime vertical CO₂ concentration difference between 1 and 36 m height is given in Figure 7 (open squares). It is always negative, being about $-4 \mu\text{mol mol}^{-1}$ in moderately stable conditions reducing to $-10 \mu\text{mol mol}^{-1}$ for $z/L > 10$. This negative sign is characteristic of all forest

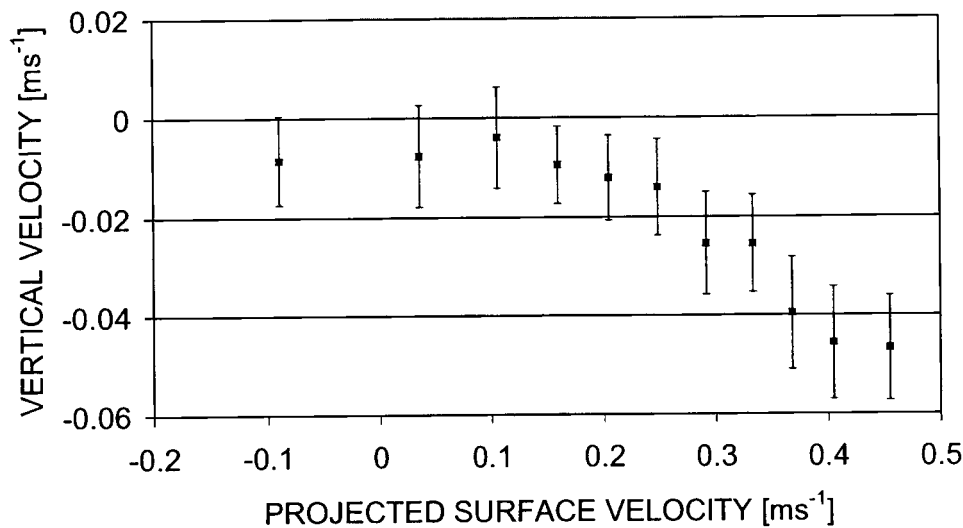


Figure 6. Evolution of the vertical velocity above the canopy with the projected surface velocity. Only the data with $z/L > 0.3$ are considered here. Each point corresponds to an average of 100 measurements. The error bars represent the standard error of the mean.

ecosystems. Indeed, at night the forest behaves as a CO₂ source, due to soil and vegetation respiration, and during periods of low turbulence the CO₂ accumulates in the lower layers of the canopy air. The combination of this gradient with the negative vertical velocity observed in these conditions (Figure 6) should give a positive vertical advection flux (i.e., a removal of CO₂ from the control volume) in stable conditions, in agreement with the observations made by Lee (1998) and Baldocchi et al. (2000). This is the case in Figure 8 where the average daily course of the vertical advection flux is presented, along with that of the other CO₂ fluxes. Being close to zero throughout the day, the advection becomes positive at night. The average values obtained at night, however, are abnormally high (from 5 to more than 10 $\mu\text{mol m}^{-2} \text{s}^{-1}$). They are more than twice the values estimated by other methods (soil respiration measurement with soil chambers (Longdoz et al., 2000), turbulence corrections (Aubinet et al., 2002)). We will show below that this discrepancy may be partly explained by the presence of horizontal advection.

The evolution at night of the horizontal gradient of CO₂ concentration with stability is also given in Figure 7 (closed squares). It is also negative, varying from zero in moderately unstable conditions to $-5 \mu\text{mol mol}^{-1}$ for $z/L > 10$. This negative sign indicates that the lower CO₂ concentration is downstream and thus that the air becomes poorer in CO₂ when flowing horizontally down the slope. Measurements of the 2002 campaign showed that such a negative horizontal gradient was observed up to about 5 m height when gravity flows develop.

This could be understood as a consequence of the entrainment process: the air descending vertically from the top of the canopy mixes with the surface flow. As

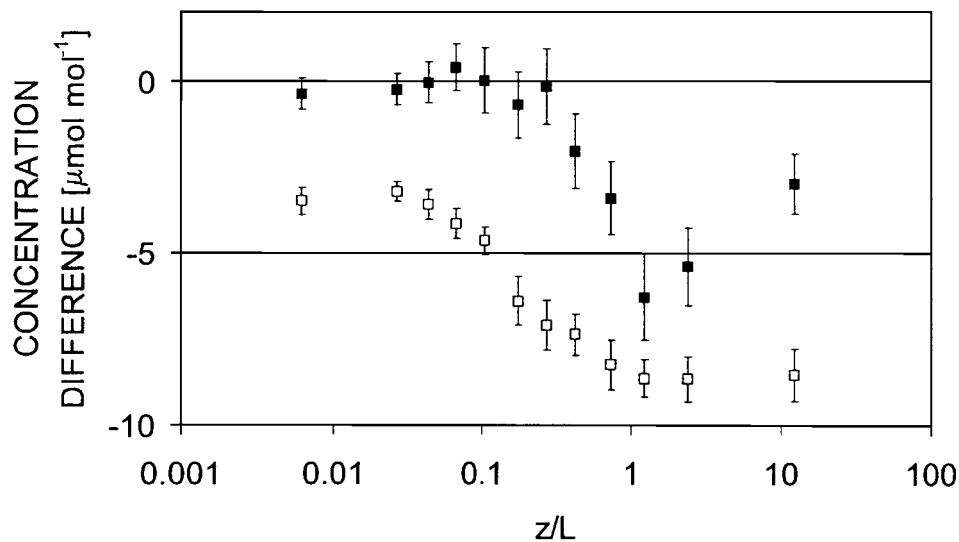


Figure 7. Evolution of the vertical and horizontal concentration gradients under stable conditions. Each point corresponds to an average of 200 measurements. The error bars represent the standard error of the mean.

the former is poorer in CO₂ than the latter, the mixing induces a dilution of the CO₂ concentration along the slope if there is no other CO₂ source. The emission of CO₂ resulting from the soil respiration in the control volume may compensate partially for this dilution. However, the soil respiration at our site is not sufficiently important to completely offset it.

The horizontal advection flux that is associated with this process is negative and thus opposed to the vertical advection. Indeed, these two fluxes are complementary and, if we supposed that the advection was the sole process at work in the control volume (i.e., the turbulent fluxes and the storage are negligible), they should cancel each other in the absence of CO₂ sources in the control volume.

The range of variation of the horizontal advection is given on Figure 8. The upper and lower limits are computed by choosing scaling heights of 3 and 10 m, respectively, in accordance with the results of the 2002 campaign. It appears that the horizontal advection is practically zero during the day and becomes negative at night as predicted above. In addition it shows that, even when estimated on the basis of the lower scaling height, its order of magnitude is similar to those of the other fluxes observed at night. This suggests that neglecting the horizontal advection in the carbon balance would introduce a significant over-estimation of the night flux. This confirms that the advection correction must be applied in a multi-dimensional perspective, as suggested by Finnigan (1999).

The results of Figure 8 also show that the day-to-day variability of the two advection terms is high. It is difficult at this stage to determine if it results from large measurement uncertainties or from a natural variability. As a result, estimates

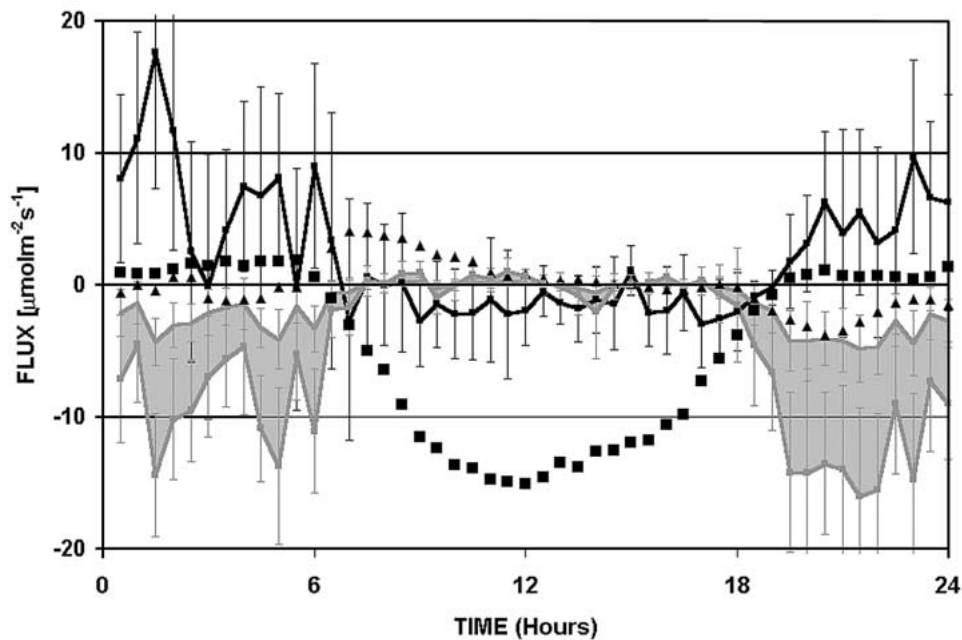


Figure 8. Average daytime evolution of eddy flux, storage, and vertical and horizontal advection during stable nights. Each point corresponds to an average of 30 measurements. The error bars represent the standard error of the mean.

of the source term cannot be deduced precisely from the carbon budget Equation (7), the uncertainty about the flux being larger than the flux itself. A discussion on the measurement error is presented in the next section.

5. Discussion on the Measurement Errors

The advection fluxes are very sensitive to measurement errors. In addition to the value of h' , the greatest sources of uncertainty are the vertical velocity at the top of the canopy for the vertical advection and the horizontal gradients of CO₂ concentrations for the horizontal advection. Indeed, these variables are generally small and close to the instrument resolution. The impact of the errors on these variables on the advection flux will be analysed below.

The vertical velocity is subjected to both systematic and random errors. In the current experiment, a systematic error appeared after the application of the rotation to the velocity vector. Above smooth terrain the vertical rotation angle should be related to the wind direction according to a sinusoidal relation or at least by a function of zero average (Lee, 1998; Paw U, 2000; Wilczak, 2000). In our case, an offset of 2° was observed in addition to a sinusoidal pattern of 1° amplitude (Figure 9). This cannot be explained by a thermally driven local circulation, as the

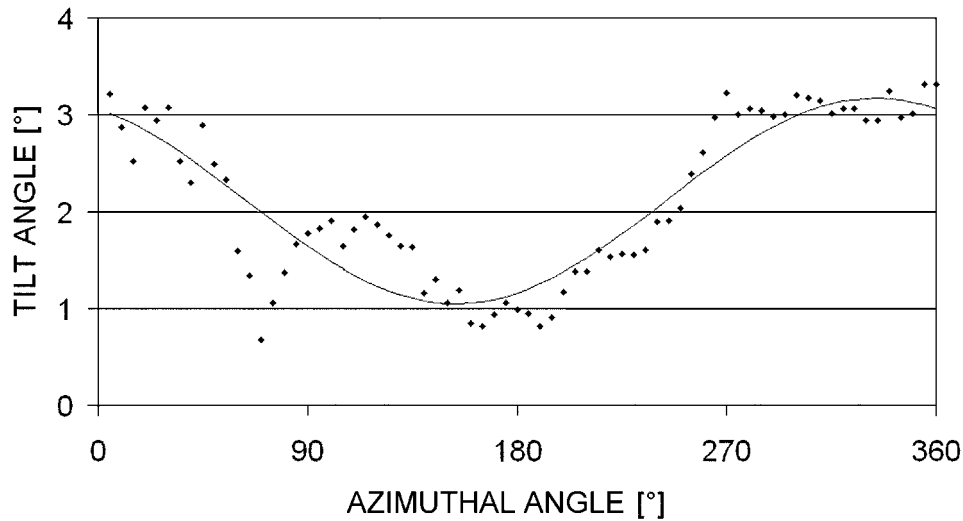


Figure 9. Evolution of the tilt angle with azimuthal angle. Points: Measurements; line: Sinusoidal regression.

measurements used to establish the relationship were selected in order to retain near-neutral periods. In addition, the topography of the Vielsalm site (a gentle, uniform slope of 3%) cannot explain such a marked preferred direction of vertical motion. We supposed, therefore, that this offset was due mainly to the anemometer or the tower structure and we included it in the correction function. We show in the Appendix that a systematic error in the vertical rotation angle would induce an error in the vertical velocity that is proportional to the horizontal component of the velocity (A4). The 2° offset would induce systematic errors on the vertical velocity up to 0.05 m s^{-1} under typical stable conditions and up to 0.11 m s^{-1} under near-neutral conditions. The resulting error in the vertical advection flux in the presence of a $10 \mu\text{mol mol}^{-1}$ vertical CO_2 concentration difference may be as high as $5 \mu\text{mol m}^{-2} \text{ s}^{-1}$. The tilt correction was applied on all the vertical velocity measurements but, as the offset value is not known with precision, a residual systematic error may remain. This error could explain the peak of vertical velocity observed between $z/L = -0.1$ and $+0.1$ in Figure 3. This is confirmed by the good correlation between the vertical and horizontal velocity at the tower top (Figure 5a). Its impact is, however, more limited in the stable range as horizontal velocities are lower. In fact, the evolution of w_h with ambient velocity in the stable range (Figure 5b) clearly differs from that in the near-neutral range.

Another important source of error arises from the horizontal CO_2 concentration gradient. In spite of the care taken to devise the system (use of the same gas analyser for all concentration measurements, use of a two-pump system to avoid pressure effects), a systematic error in the horizontal gradient was observed, as revealed by the frequency distribution of dc/dx (Figure 10). Indeed, the most

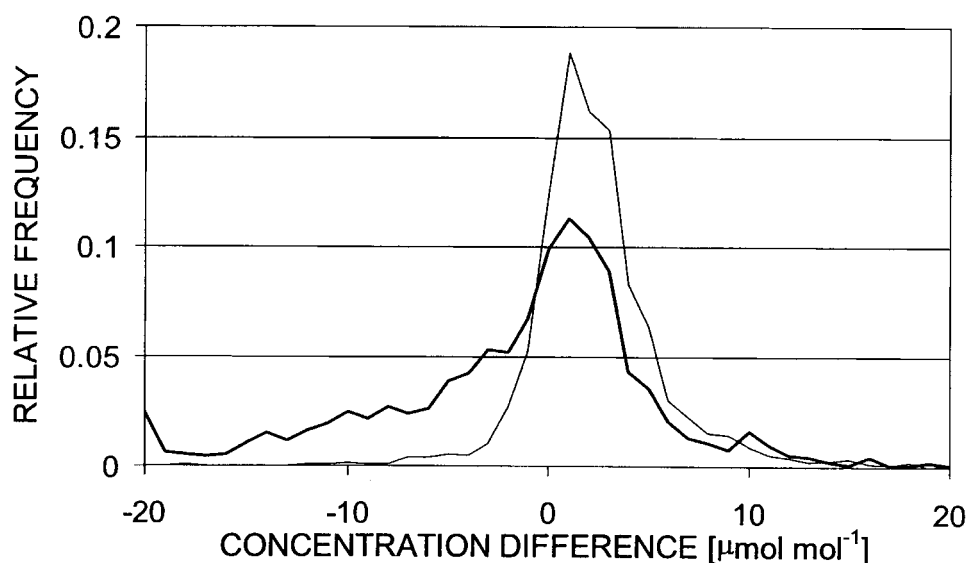


Figure 10. Horizontal concentration difference frequency distribution. Solid line: 1435 measurements in near-neutral conditions ($-0.1 < z/L < 0.1$); dotted line: 924 measurements under stable conditions ($z/L > 0.35$).

frequent difference observed under unstable and near-neutral conditions was about $2.5 \mu\text{mol mol}^{-1}$. As this difference was observed over a large range of wind speed and directions it is unlikely to correspond to a real advection process; more probably, it results from a systematic error due to the measurement system or to the sampling point positioning. In addition, the values of the advection flux that would be deduced from these gradients would become unrealistic: under typical advective conditions (horizontal velocity at the surface: 0.4 m s^{-1}), such concentration differences would induce a systematic error between 2.4 and $8 \mu\text{mol m}^{-2} \text{ s}^{-1}$ according to the scaling height value. For these reasons, the horizontal concentration differences used for the advection computation were corrected by assuming the zero to correspond with the maximum frequency. It appears then that negative concentration differences were more frequently observed in the stable than in the unstable/near-neutral range (Figure 10). The concentration differences presented in Figure 7 were also corrected this way.

6. Conclusions

The measurements of wind velocities and CO₂ concentrations taken at the Vielsalm site allowed us to draw a pattern of the flow that develops under stable conditions on a single slope.

The measurements of the surface wind velocity showed that gravity flows develop under stable conditions. Such flows were frequently observed over steep

slopes (Horst and Doran, 1986; Clements et al., 1989) and less frequently over slight slopes such as those at Vielsalm (Mahrt and Larsen, 1990).

Our measurements also showed that the vertical velocity at the top of the canopy was well correlated with the surface velocity under stable conditions. This suggests that these variables constitute two facets of the same global mechanism: first, surface radiative cooling acting upstream to the site creates a gravity flow that flows through the forest understorey; secondly, this horizontal flow provokes, by entrainment, a vertical flow from the top of the trees to the soil.

The measurements of CO₂ concentration showed that there was a horizontal CO₂ concentration gradient during these events, and that the lower concentration was always at the downstream point. This is explained by the mass conservation equation: the air descending vertically from the canopy top mixes with the surface flow. As the former is poorer in CO₂ than the latter, it would induce a dilution of the CO₂ along the slope that is not entirely compensated by the CO₂ produced by the sources.

The CO₂ advection flux resulting from this mechanism may be separated into two components: a vertical component resulting from vertical velocity and concentration gradient, and a horizontal component resulting from the gravity flow and the horizontal gradient. Our measurements suggest that the two components of advection are large and opposite. This shows that the night flux correction based on the inclusion of advection into the carbon budget equation should take the two components into account. In particular, it suggests that the Lee (1998) correction is inappropriate on single sloping sites since it takes account only of the vertical component. Indeed, the correction term would be over-estimated and would lead to an under-estimation of the long-term carbon sequestration. On flat sites or on more complex terrains, the situation is more complicated. Nevertheless, according to the mass conservation equation, a dilution effect should appear every time that the vertical velocity is downward. In these cases, the horizontal component of the advection should be significant, but it would be very difficult to estimate as the direction of the horizontal flow is not clearly defined.

The main problem that remains at this stage is the lack of accuracy of advection measurements. Indeed, errors on the vertical velocity, on the vertical profile of horizontal velocity and on the horizontal concentration gradients are significant and do not allow a reasonable estimation to be made of the total advection flux. Thus, we consider that it is not possible at this stage to routinely apply the advection correction to the CO₂ fluxes at night. A careful error analysis and a better design of the system should be performed in order to reduce these errors.

Acknowledgements

This research was supported by the European Commission, Programme Environment and Climate, project CARBOEUROFLUX under contract EVK2-CT-1999-

00032 and by the Belgian Fonds National de la Recherche Scientifique (Dossier 2.4526.01). We acknowledge Prof. Larry Mahrt and an unknown referee for giving constructive comments and Julie Lescaut for encouraging us to make night observations.

Appendix A

The vertical component of the velocity obtained after the second rotation, w_2 , is expressed in terms of the rotated velocity components, u_1 and w_1 , as (Aubinet et al., 2000):

$$w_2 = -u_1 \sin \phi + w_1 \cos \phi, \quad (\text{A1})$$

where ϕ is the angle of the second rotation. The error on w_2 , ε_{w_2} may thus be derived from (A1) as (Taylor, 1997):

$$\varepsilon_{w_2} = \sqrt{\varepsilon_{u_1}^2 \sin^2 \phi + \varepsilon_{\sin \phi}^2 u_1^2 + \varepsilon_{w_1}^2 \cos^2 \phi + \varepsilon_{\cos \phi}^2 w_1^2}, \quad (\text{A2})$$

where ε_{u_1} , ε_{w_1} , $\varepsilon_{\sin \phi}$, $\varepsilon_{\cos \phi}$ are the errors in, respectively, the horizontal and the vertical component of the velocity and the sine and cosine of the second rotation angle. The latter, however, is generally small (some hundredths of radians) so that: $\sin \phi \approx \phi$, $\cos \phi \approx 1$, and thus, $\varepsilon_{\sin \phi} \approx \varepsilon_\phi$ and $\varepsilon_{\cos \phi} \approx 0$. With these approximations, (A2) becomes:

$$\varepsilon_{w_2} \approx \sqrt{\varepsilon_{u_1}^2 \phi^2 + \varepsilon_\phi^2 u_1^2 + \varepsilon_{w_1}^2}. \quad (\text{A3})$$

In addition, the errors on the horizontal and the vertical velocity are generally some orders of magnitude lower than u_1 so that, if we consider the error on the second rotation angle to be of the same order of magnitude as the angle itself, the first and third terms in the square root can be neglected compared to the second. We have therefore:

$$\varepsilon_{w_2} \approx \varepsilon_\phi u_1, \quad (\text{A4})$$

which shows that, to the first order, the impact of an error on the second rotation angle is proportional to the horizontal velocity.

References

- Aubinet, M., Chermanne, B., Vandenhaute, M., Longdoz, B., Yernaux, M., and Laitat, E.: 2001, 'Long Term Carbon Dioxide Exchange above a Mixed Forest in the Belgian Ardennes', *Agric. For. Meteorol.* **108**, 293–315.

- Aubinet, M., Grelle A., Ibrom, A., Rannik, Ü., Moncrieff, J., Foken, T., Kowalski, A. S., Martin, P. H., Berbigier, P., Bernhofer, Ch., Clement, R., Elbers, J., Granier, A., Grünwald, T., Morgenstern, K., Pilegaard, K., Rebmann, C., Snijders, W., Valentini, R., and Vesala, T.: 2000, 'Estimates of the Annual Net Carbon and Water Exchange of Forests: The EUROFLUX Methodology', *Adv. Ecol. Res.* **30**, 113–175.
- Aubinet, M., Heinesch, B., and Longdoz, B.: 2002, 'Estimation of the Carbon Sequestration by a Heterogeneous Forest: Night Flux Corrections, Heterogeneity of the Site and Inter-Annual Variability', *Global Change Biol.* **8**, 1053–1072.
- Baldocchi, D., Finnigan, J., Wilson, K., Paw U, K. T., and Falge, E.: 2000, 'On Measuring Net Ecosystem Carbon Exchange over Tall Vegetation on Complex Terrain', *Boundary-Layer Meteorol.* **96**, 257–291.
- Black, T. A., den Hartog, G., Neumann, H. H., Blanken, P. D., Yang, P. C., Russell, C., Nesic, Z., Lee, X., Chen, S., Staebler, R., and Novak, M. D.: 1996, 'Annual Cycles of Water Vapour and Carbon Dioxide Fluxes in and above a Boreal Aspen Forest', *Global Change Biol.* **2**, 219–229.
- Clements, W. E., Archuleta, J. A., and Hoard, D. E.: 1989, 'Mean Structure of the Nocturnal Drainage Flow in a Deep Valley', *J. Appl. Meteorol.* **28**, 457–462.
- Finnigan, J.: 1999, 'A Comment on the Paper by Lee (1998): On Micrometeorological Observations of Surface-Air Exchange over Tall Vegetation', *Agric. For. Meteorol.* **97**, 55–64.
- Finnigan, J., Clement, R., Mahli, Y., Leuning, R., and Cleugh, H.: 2003, 'A Re-Evaluation of Long-Term Flux Measurement Techniques. Part 1: Averaging and Coordinate Rotation', *Boundary-Layer Meteorol.* **107**, 1–48.
- Goulden, M. L., Munger, J. W., Fan, S.-M., Daube, B. C., and Wofsy, S. C.: 1996, 'Measurements of Carbon Sequestration by Long-Term Eddy Covariance: Methods and a Critical Evaluation of Accuracy', *Global Change Biol.* **2**, 169–182.
- Greco, S. and Baldocchi D.: 1996, 'Seasonal Variations of CO and Water Vapour Exchange Rates over a Temperate Deciduous Forest', *Global Change Biol.* **2**, 183–197.
- Horst T. W. and Doran J. C.: 1986, 'Nocturnal Drainage Flow on Simple Slopes', *Boundary-Layer Meteorol.* **12**, 1072–1075.
- Kotsovinos, N. E. and List E. J.: 1977, 'Plane Turbulent Buoyant Jets. Part I. Integral Properties', *J. Fluid Mech.* **81**, 25–44.
- Laitat E., Chermanne B., and Portier B.: 1999, 'Biomass, Carbon and Nitrogen Allocation in Open Top Chambers under Ambient and Elevated CO₂ and in a Mixed Forest Stand. A Tentative Approach for Scaling up from the Experiments of Vielsalm', in R. J. M. Ceulemans, F. Veroustraete, V. Gond, and J. B. H. F. Van Rensbergen (eds.), *Forest Ecosystem Modelling, Upscaling and Remote Sensing*, SPB Academic Publishing, The Hague, The Netherlands, pp. 33–60.
- Lee, S. L. and Emmons H. W.: 1961, 'A Study of Natural Convection above a Line Fire', *J. Fluid Mech.* **11**, 353–368.
- Lee, X.: 1998, 'On Micrometeorological Observations of Surface-Air Exchange over Tall Vegetation', *Agric. For. Meteorol.* **91**, 39–49.
- Lindroth, A., Grelle A., and Moren, A.-S.: 1998, 'Long-Term Measurements of Boreal Forest Carbon Balance Reveal Large Temperature Sensitivity', *Global Change Biol.* **4**, 443–450.
- Longdoz, B., Yernaux M., and Aubinet, M.: 2000, 'Soil CO₂ Efflux Measurements in a Mixed Forest: Impact of Chamber Disturbances, Spatial Variability and Seasonal Evolution', *Global Change Biol.* **6**, 907–917.
- Mahrt, L.: 1998, 'Flux Sampling Errors for Aircraft and Towers', *J. Atmos. Oceanic Tech.* **15**, 416–429.
- Mahrt, L. and Larsen S.: 1990, 'Relation of Slope Winds to the Ambient Flow over Gentle Terrain', *Boundary-Layer Meteorol.* **53**, 93–102.
- Manins, P. C. and Sawford B. L.: 1979, 'A Model of Katabatic Winds', *J. Atmos. Sci.* **36**, 619–630.
- Massman, W. J. and Lee X.: 2002, 'Eddy Covariance Flux Corrections and Uncertainties in Long Term Studies of Carbon and Energy Exchanges', *Agric. For. Meteorol.* **113**, 121–144.

- Moncrieff, J. B., Malhi, Y., and Leuning, R.: 1996, 'The Propagation of Errors in Long-Term Measurements of Land Atmosphere Fluxes of Carbon and Water', *Global Change Biol.* **2**, 231–240.
- Moncrieff, J. B., Massheder, J. M., de Bruin, H., Elbers, J., Friborg, T., Heusinkveld, B., Kabat, P., Scott, S., Soegaard, H., and Verhoef, A.: 1997, 'A System to Measure Surface Fluxes of Momentum, Sensible Heat, Water Vapour and Carbon Dioxide', *J. Hydrol.* **188–189**, 589–611.
- Paw U, K. T., Baldocchi, D. D., Meyers, T. P., and Wilson, K. B.: 2000, 'Correction of Eddy-Covariance Measurements Incorporating Both Advective Effects and Density Fluxes', *Boundary-Layer Meteorol.* **97**, 487–511.
- Pilegaard, K., Hummelshoj, P., Jensen, N. O., and Chen, Z.: 2001, 'Two Years of Continuous CO₂ Eddy-Flux Measurements over a Danish Beech Forest', *Agric. For. Meteorol.* **107**, 29–41.
- Schmid, H. P., Grimmond, S., Cropley, F., Offerle, B., and Su, H. B.: 2000, 'Measurements of CO₂ and Energy Fluxes over a Mixed Hardwood Forest in the Mid-Western United States', *Agric. For. Meteorol.* **103**, 357–374.
- Taylor, J. R.: 1997, *An Introduction to Error Analysis*, University Science Books, Sausalito, CA, 327 pp.
- Turnipseed, A. A., Blanken, P. D., Anderson, D. E., and Monson, R. K.: 2002, 'Energy Budget above a High-Elevation Subalpine Forest in Complex Topography', *Agric. For. Meteorol.* **110**, 177–201.
- Valentini, R., Matteucci, G., Dolman, H., Schultze, E. D., Rebmann, C., Moors, E. J., Granier, A., Gross, P., Jensen, N. O., Pilegaard, K., Lindroth, A., Grelle, A., Bernhofer, C., Grünwald, T., Aubinet, M., Ceulemans, R., Kowalsky, A. S., Vesala, T., Rannik, U., Berbigier, P., Lousteau, D., Guomundsson, J., Thorgeirsson, H., Ibrom, A., Morgenstern, K., Clement, R., Moncrieff, J., Montagnani, L., Minerbi, S., and Jarvis, P. G.: 2000, 'Respiration as the Main Determinant of Carbon Balance in European Forests', *Nature* **404**, 861–865.
- Wang, S., Yernaux, M., and Deltour, J. 1999, 'A Networked Two-Dimensional Sonic Anemometer System for the Measurement of Air Velocity in Greenhouses', *J. Agric. Eng. Res.* **73**, 189–197.
- Wilczack, J., Oncley, S. P., and Stage, S. A.: 2001, 'Sonic Anemometer Tilt Correction Algorithms', *Boundary-layer Meteorol.* **99**, 127–150.
- Wofsy, S. C., Goulden, M. L., Munger, J. W., Fan, S.-M., Bakwin, P. S., Daube, B. C., Bassow, S. L., and Bazzaz, F. A.: 1993, 'Net Exchange of CO in a Mid-Latitude Forest', *Science* **260**, 1314–1317.

